

Er³⁺-activated nanocomposite photonic glasses and confined structures

C. Armellini^a, A. Chiappini^a, A. Chiasera^{a,*}, M. Ferrari^a, Y. Jestin^a, E. Moser^b, G. Nunzi Conti^{c,d}, S. Pelli^d, A. Quandt^{a,e}, G.C. Righini^{d,f}, C. Tosello^b

^aCNR-IFN, Institute of Photonics and Nanotechnology, CSMFO Group, via Sommarive 14, 38050 Povo-Trento, Italy

^bPhysics Department, Trento University, CSMFO Group, via Sommarive 14, 38050 Povo-Trento, Italy

^cCentro Fermi, Complesso del Viminale, 00184 Roma, Italy

^dCNR-IFAC, Nello Carrara Institute of Applied Physics, via Madonna del Piano 10, 50019 Sesto Fiorentino-Firenze, Italy

^eInstitut fuer Physik, Universitaet Greifswald, Hausdorff-Str. 6, 17489 Greifswald, Germany

^fCNR, Materials and Devices Department, via dei Taurini 19, 00185 Roma, Italy

ARTICLE INFO

Article history:

Available online 8 May 2008

Keywords:

Nanocomposites glasses

Erbium

Sol-gel

1D photonic crystals

Photoluminescence

ABSTRACT

This paper reports about recent advances in optical nanomaterials and planar microcavities. Bottom-up fabrication, optical and spectroscopic assessment of Er³⁺-activated SiO₂-HfO₂ waveguide glass ceramic are presented. Concerning confined structures, the rf sputtering based fabrication of an Er³⁺-activated microcavity with a quality factor of 171 using oxide-based dielectric materials is demonstrated.

© 2008 Elsevier B.V. All rights reserved.

1. Introduction

The last decade has seen a remarkable increase in the experimental efforts to control and enhance the emission properties of various emitters, in particular Er³⁺-ions, by tailoring the dielectric surrounding of the sources. With this aim, several approaches, using nanocomposite materials [1–3] and specific geometries, such as planar interfaces [4], photonic crystals [5,6], solid state planar microcavities [5,7,8], dielectric nanospheres [9,10], and spherical microresonators [11,12], have been proposed, which open new possibilities in the field of basic as well as applied physics, and other areas including Information Communication Technologies, Health and Biology, Structural Engineering, and Environment Monitoring Systems.

Nanostructured materials have sparked great interest among the academic and industrial communities over the past decade, due to the remarkable variations in the fundamental electrical, optical and magnetic properties that occur during the transition from a bulk “homogeneous” material to a particle or a cluster within the 1–100 nm range. Moreover, the possibility to develop optically confined structures would allow for novel optical components, and the glass-based planar technology appears to be consolidated enough to allow the design of complex optical de-

vices [1]. A more effective control of luminescence properties may be achieved by rare earth-activated microcavities, which represent a particular class of photonic crystals [5].

The aim of this paper is to give an overview of the advances in glass-based photonic systems, where light confinement or the presence of nanostructured hosts induces an enhancement of optical and/or spectroscopic properties of the rare earth ions. In particular, the following topics will be highlighted: (i) dielectric 1D photonic band gap structures or planar microcavities, characterized by a high quality factor *Q*; (ii) Er³⁺-activated glass ceramics planar waveguides obtained by innovative bottom-up technique.

2. Dielectric 1D microcavity

In this section we report on an Er³⁺-codoped all-dielectric microcavity fabricated by rf sputtering (RFS) and operating at 1544 nm.

The microcavity consists of a SiO₂ half-wave layer inserted between two Bragg reflectors composed of a stack of six pairs of alternated SiO₂ and TiO₂ quarter-wave layers. Each SiO₂ layer is activated with 0.3 at% of Er³⁺ ions, as measured by energy dispersive spectroscopy (EDS) using a Noran Instruments mod. Voyager apparatus. The refractive index at 1542 nm of the silica and titania layers, measured by m-line spectroscopy on the single films, was 1.444 ± 0.002 and 2.30 ± 0.02 , respectively. To increase the reflection coefficient of the distributed Bragg reflectors (DBRs), the index

* Corresponding author.

E-mail address: achiaser@science.unitn.it (A. Chiasera).

contrast between the two materials should be as large as possible, and TiO_2 and SiO_2 have been chosen [5]. The samples were deposited on silicon and silica substrates. The sample deposited on silicon was employed for SEM measurements. The sample deposited on a silica substrate was employed for transmittance and photoluminescence measurements. In order to improve the adhesion of the films, the substrates were cleaned inside the RFS deposition chamber by removing some atomic layers just before the deposition procedure: in this pre-sputtering stage the face of the substrates is exposed to the plasma for 10 min. Sputtering deposition of the films was performed by sputtering alternatively a 4" titania target and a 4" silica target on which metallic erbium pieces were placed. The deposition time required to reach the appropriate thicknesses of the Bragg grating layers was 14 min 15 s for the titania target and 11 min 15 s for the silica target. The deposition time required to reach the appropriate thickness of the silica defect layer leading to a cavity resonance centered at 1.5 μm , was 25 min. The residual pressure, before deposition, was about 2×10^{-7} mbar. During the deposition process the substrates were not heated. The sputtering occurred with an Ar pressure of 5×10^{-3} mbar; the applied rf power was 150 W, with a reflected power of 16 W and 0 W for silica and titania targets, respectively.

A SEM image of the cross section of the cavity fabricated with this protocol is shown in Fig. 1. The dark regions correspond to the SiO_2 layers and the bright ones to the TiO_2 layers. It is possible to identify the defect layer and the two Bragg reflectors. The SEM image allowed us to measure a thickness of 210 ± 5 nm and 195 ± 5 nm for the silica and titania layers of the Bragg mirrors, and a thickness of 490 ± 5 nm for the SiO_2 defect layer.

The transmittance spectrum of the cavity, obtained by using a Varian-Carry spectrophotometer, is shown in Fig. 2. The spectral reflection range, i.e. the stop band, lies from 1350 to 1850 nm. A sharp peak in the transmittance spectrum appears at 1544 nm. It corresponds to the cavity resonance wavelength related to the half wave layer inserted between the Bragg mirrors.

Fig. 3 compares the $^4\text{I}_{13/2} \rightarrow ^4\text{I}_{15/2}$ PL spectrum of the cavity activated by Er^{3+} ions to the PL spectrum of the single Er^{3+} -doped SiO_2 active layer without Bragg mirrors. Both the cavity and no-cavity structures were excited with the 514 nm line of an Ar^+ ion laser with an excitation power of 100 mW. The luminescence was dispersed by a 320 mm single-grating monochromator with a resolution of 1 nm. The light was detected using a Hamamatsu photomultiplier tube and standard lock-in technique. For this analysis, the samples are fixed on a rotating holder. The PL from the cavity and from the Er^{3+} -doped single SiO_2 layer were detected at 5° from the normal on the samples, with a solid angle of 10^{-1} steradian. The erbium emission from the no-cavity single SiO_2 active layer is centered at 1538 nm with a full width at half maximum (FWHM) of 28 nm and exhibits the characteristic shape of erbium ion emission in silica glass [13]. The cavity

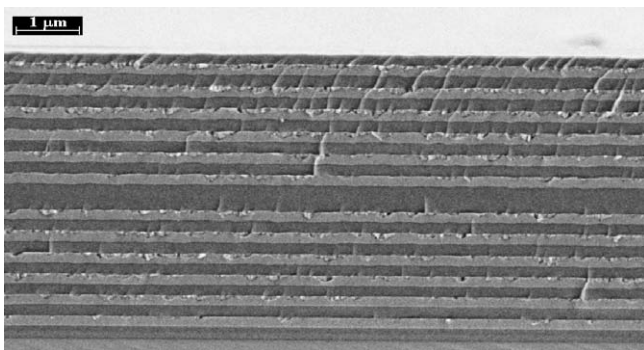


Fig. 1. Cross section image of the sample obtained using scanning electron microscopy. The bright and the dark areas are TiO_2 and SiO_2 layers, respectively [5].

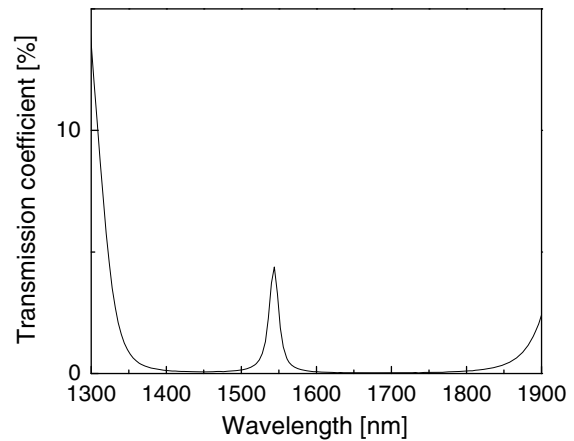


Fig. 2. Transmittance spectrum of the cavity with a six doublets Bragg mirror. The stop band extends from 1350 to 1850 nm. The cavity resonance corresponds to the sharp maximum at the center of the transmission window. The incident light is non-polarized.

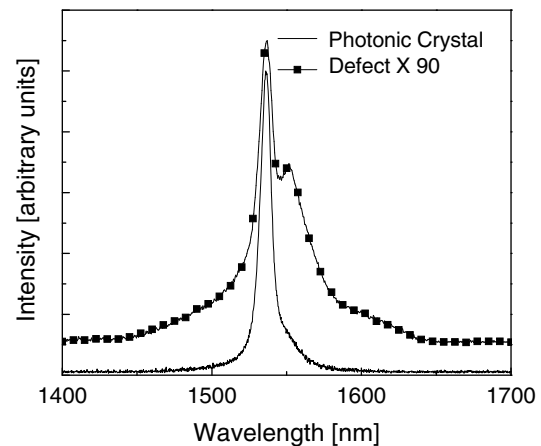


Fig. 3. $^4\text{I}_{13/2} \rightarrow ^4\text{I}_{15/2}$ photoluminescence spectra of the cavity activated by Er^{3+} ion (1D photonic crystal) and of the single Er^{3+} -doped SiO_2 active layer without Bragg mirrors (defect). The light is recorded at 5° from the normal with respect to the samples, and upon excitation at 514.5 nm.

resonance is strongly dependent on the detection angle [14]. For a detection angle of 5° , the cavity resonance corresponds to the maximum of the erbium PL of the no-cavity SiO_2 active layer. The peak luminescence intensity of Er^{3+} ions is enhanced by a factor 90, with respect to the no-cavity case at the same wavelength. The Er^{3+} $^4\text{I}_{13/2} \rightarrow ^4\text{I}_{15/2}$ PL line shape is strongly modified by the cavity, and the Er^{3+} emission is enhanced when the wavelength corresponds to the cavity resonant mode, but weakens for the other emission wavelengths. A sharp line is observed for PL spectrum from the cavity, as shown in Fig. 3. The FWHM is 9 nm, corresponding to a quality factor of the cavity, Q , equal to 171, assuming the absence of photon re-absorption [7,15].

3. Bottom-up glass-ceramic planar waveguides

Ceramic glassy materials may be a valid alternative to control the chemical parameters of the rare earth components, thus avoiding undesirable effects like clustering. Using a bottom-up approach $\text{SiO}_2\text{-HfO}_2\text{:Er}^{3+}$ glass-ceramic planar waveguides were realized by following the described protocol: (1) preparation of a colloidal suspension of HfO_2 nanoparticles, starting from a HfOCl_2 solution

in ethanol and using a reflux technique; (2) separation of HfO₂ nanoparticles from the colloidal suspension; (3) preparation of a solution of TEOS, alcohol, deionised water and hydrochloric acid prehydrolyzed for 1 h at 65 °C, in which has been added the hafnia precursor HfOCl₂ in order to obtain a final solution with a molar ratio Si/Hf = 80/20; 4) to this solution Er(NO₃)₃·5H₂O has been added with a molar concentration Er/(Si+Hf) = 1 as well as hafnia nanoparticles, in order to obtain 2.5 mol% of nanoparticles in the solution [1]. Nanocomposite planar waveguides were produced by dip-coating the final solution on a SiO₂ substrate, stabilized by a thermal treatment at 900 °C in air for 22 h (see Table 1).

After the introduction of hafnia nanoparticles in the silica–hafnia sol, a HRTEM image (Fig. 4) of the produced waveguide has been made, which shows nanocrystals of about 3–4 nm in size homogeneously scattered over the amorphous matrix. This shows the feasibility of a bottom-up approach for the production of nanocomposite waveguides.

The EDS analysis has confirmed that the nanocrystals are composed of hafnium oxide. Fig. 5 compares the ⁴I_{13/2} → ⁴I_{15/2} PL spectrum of the waveguide glass-ceramic (WGC) activated by Er³⁺ ions, and the PL spectrum of a silica–hafnia Er³⁺-activated waveguide without nanocrystals (WG). The ⁴I_{13/2} → ⁴I_{15/2} photoluminescence spectrum of the nanocomposite waveguide indicates that the ordering of the local environment limits the inhomogeneous broadening typical of glassy structural environments. In fact, the FWHM is 27 nm for the glass ceramic as compared to the 45 nm measured for the amorphous system [1]. We can assume that the thermal treatment at 900 °C, which does not damage the surface of the film, has promoted the migration of erbium ions towards the hafnia nanocrystals [16]. The lifetime of the metastable level ⁴I_{13/2} has been measured at 1532 nm. The decay curve presents a single exponential behaviour with a lifetime of 5.6 ms, as compared to 4.5 ms measured for the amorphous waveguide [1]. Because the hafnia cut-off frequency is around 700 cm⁻¹, the main effect of the presence of nanocrystals is a reduction of the nonradiative processes, thus inducing a lengthening of the lifetime for the metastable level ⁴I_{13/2}. The bot-

Table 1

Annealing temperature, size of nanocrystals, attenuation coefficient, and ⁴I_{13/2} lifetime of the Er³⁺-activated SiO₂–HfO₂ glass ceramic planar waveguide

Thermal treatment (°C)	900
Crystallites size (±1 nm)	3–4
Losses at 1542 nm (±0.3 dB/cm)	0.3
Lifetime at 1532 nm (ms)	5.6

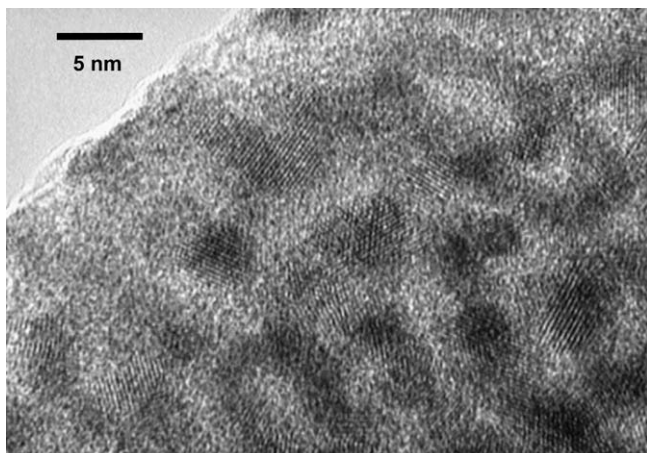


Fig. 4. HRTEM image of the glass-ceramic waveguide showing HfO₂ nanocrystals scattered over the amorphous matrix.

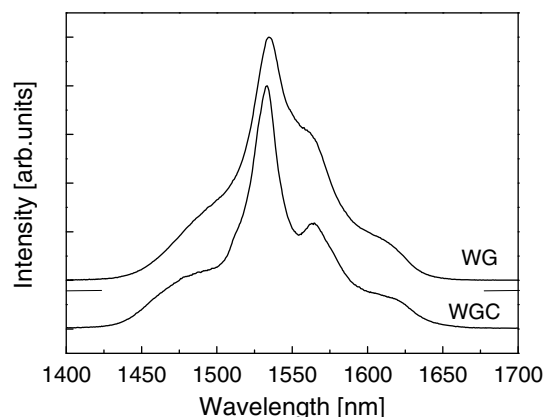


Fig. 5. Room temperature luminescence spectra of the ⁴I_{13/2} → ⁴I_{15/2} transition of Er³⁺ ions for a glass-ceramic waveguide (WGC) and an amorphous planar waveguide (WG), obtained by exciting the TE₀ mode at 514.5 nm.

tom-up waveguide shows excellent propagation properties at 1.5 μm with losses around 0.3 dB/cm, which will make it a suitable component for low losses amplifier in the C band of telecommunication. It is important to note that the bottom-up method will allow for a clear amelioration of the optical properties of glass-ceramic waveguides as compared to waveguides obtained by the standard top-down method. The top-down method requires a high thermal treatment at 1000 °C, to grow nanocrystals in the matrix, and it induces optical losses of 1 dB/cm at 1542 nm, caused by a degradation of the waveguide surface [17].

4. Conclusions

Using the rf sputtering technique, we fabricated via an Er³⁺-activated microcavity with a quality factor of 171 using Er³⁺-doped-SiO₂ and TiO₂ thin films. The transmittance spectrum shows a cavity resonance centered at 1544 nm with a stop band from 1350 to 1850 nm. Er³⁺ luminescence enhancement of 90 times was observed, caused by the cavity effect.

Concerning glass ceramics, we have defined a fabrication protocol by sol–gel route of rare earth activated glass-ceramic planar waveguides. The waveguides have been realized using a bottom-up technique. Optical measurements have evidenced that glass ceramics containing nanocrystals of about 3 nm may exhibit a low attenuation coefficient of 0.3 dB/cm at 1542 nm.

Acknowledgements

The work reported in this paper was partially supported by PAT (2004–2006) FAPVU, CNR-CNRS 2005–2007, and PAT FaStFAL (2007–2009) research projects.

References

- [1] Y. Jestin, C. Armellini, A. Chiasera, A. Chiappini, M. Ferrari, E. Moser, R. Retoux, G.C. Righini, Appl. Phys. Lett. 91 (2007) 071909-1/3.
- [2] V.K. Tikhomirov, D. Furniss, A.B. Seddon, I.M. Reaney, M. Beggiora, M. Ferrari, M. Montagna, R. Rolli, Appl. Phys. Lett. 81 (2002) 1937.
- [3] R. Serna, A. Suarez-Garcia, M. Jiménez de Castro, C.N. Afonso, Appl. Surf. Sci. 247 (2005) 8.
- [4] E. Snoeks, A. Lagendijk, A. Polman, Phys. Rev. Lett. 74 (1995) 2459.
- [5] A. Chiasera, R. Belli, S.N.B. Bhaktha, A. Chiappini, M. Ferrari, Y. Jestin, E. Moser, G.C. Righini, C. Tosello, Appl. Phys. Lett. 89 (2006) 171910/1.
- [6] J. Kalkman, E. de Bres, A. Polman, Y. Jun, D.J. Norris, D.C. 't Hart, J.P. Hoogenboom, A. van Blaaderen, J. Appl. Phys. 95 (2004) 2297.
- [7] J. Bellessa, S. Rabaste, J.C. Plenet, J. Dumas, J. Mugnier, O. Marty, Appl. Phys. Lett. 79 (2001) 2142.
- [8] A.M. Vredenberg, N.E. Hunt, E.F. Schubert, D.C. Jacobson, J.M. Poate, G.J. Zydzik, Phys. Rev. Lett. 71 (1992) 517.

- [9] H. Schniepp, V. Sandoghdar, *Phys. Rev. Lett.* 89 (2002) 257403-1/4.
- [10] A. Chiappini, C. Armellini, A. Chiasera, M. Ferrari, Y. Jestin, M. Mattarelli, M. Montagna, E. Moser, G. Nunzi Conti, S. Pelli, G.C. Righini, M. Clara Gonçalves, Rui M. Almeida, *J. Non-Cryst. Solids* 353 (2007) 674.
- [11] L. Yang, T. Carmon, B. Min, S.M. Spillane, K.J. Vahala, *Appl. Phys. Lett.* 86 (2005) 091114-1/3.
- [12] G.C. Righini, C. Armellini, A. Chiasera, Y. Jestin, M. Ferrari, A. Chiappini, M. Montagna, C. Arfuso Duverger, P. Féron, S. Berneschi, M. Brenci, G. Nunzi Conti, S. Pelli, C. Gonçalves, Rui M. Almeida, *Glass Technol. – Eur. J. Glass Sci. Technol. Part A* 48 (2007) 200.
- [13] W.J. Miniscalco, *J. Lightwave Technol.* 9 (1991) 234.
- [14] K.M. Chen, A.W. Sparks, H.-C. Luan, D.R. Lim, K. Wada, L.C. Kimerling, *Appl. Phys. Lett.* 75 (1999) 3805.
- [15] H. Rigneault, C. Amra, S. Robert, C. Begon, F. Lamarque, B. Jacquier, P. Moretti, A.M. Jurdyc, A. Belarouci, *Opt. Mater.* 11 (1999) 167.
- [16] W.C. Liu, D. Wu, A.D. Li, H.Q. Ling, Y.F. Tang, N.B. Ming, *Appl. Surf. Sci.* 191 (2002) 181.
- [17] Y. Jestin, C. Armellini, A. Chiappini, A. Chiasera, M. Ferrari, C. Goyes, M. Montagna, E. Moser, G. Nunzi Conti, S. Pelli, R. Retoux, G.C. Righini, G. Speranza, *J. Non-Cryst. Solids* 353 (2007) 494.